HHS Public Access

Author manuscript

Brain Behav Immun. Author manuscript; available in PMC 2021 July 01.

Published in final edited form as:

Brain Behav Immun. 2020 July ; 87: 840–851. doi:10.1016/j.bbi.2020.03.019.

Toll-like receptor 7 contributes to neuropathic pain by activating NF-κB in primary sensory neurons

Long He[1,*], **Guang Han**[1,*], **Shaogen Wu**[1], **Shibin Du**[1], **Yang Zhang**[1], **Weili Liu**[1], **Baochun Jiang**[1], **Luyao Zhang**[1], **Shangzhou Xia**[1], **Shushan Jia**[1], **Stephen Hannaford**[1], **Ying Xu**[2], **Yuan-Xiang Tao**[1,3,4,†]

[1]Department of Anesthesiology, New Jersey Medical School, Rutgers, The State University of New Jersey, Newark, NJ 07103, USA

[2]Department of Pharmaceutical Sciences, School of Pharmacy and Pharmaceutical Sciences, The State University of New York, Buffalo, NY14214, USA

[3]Department of Physiology, Pharmacology & Neuroscience, New Jersey Medical School, Rutgers, The State University of New Jersey, Newark, NJ 07103, USA

[4]Department of Cell Biology & Molecular Medicine, New Jersey Medical School, Rutgers, The State University of New Jersey, Newark, NJ 07103, USA

Abstract

Toll like receptor 7 (TLR7) is expressed in neurons of the dorsal root ganglion (DRG), but whether it contributes to neuropathic pain is elusive. We found that peripheral nerve injury caused by ligation of the fourth lumbar (L_4) spinal nerve (SNL) or chronic constriction injury of sciatic nerve led to a significant increase in the expression of TLR7 at mRNA and/or protein levels in mouse injured DRG. Blocking this increase through microinjection of the adeno-associated virus (AAV) 5 expressing TLR7 shRNA into the ipsilateral L_4 DRG alleviated the SNL-induced mechanical, thermal and cold pain hypersensitivities in both male and female mice. This microinjection also attenuated the SNL-induced increases in the levels of phosphorylated extracellular signal-regulated kinase ½ (p-ERK1/2) and glial fibrillary acidic protein (GFAP) in L_4 dorsal horn on the ipsilateral side during both development and maintenance periods. Conversely, mimicking this increase through microinjection of AAV5 expressing full-length TLR7 into unilateral $L_{3/4}$ DRGs led to elevations in the amounts of p-ERK1/2 and GFAP in the dorsal horn, augmented responses to

†Corresponding author: Yuan-Xiang Tao, MD, PhD, Department of Anesthesiology, New Jersey Medical School, Rutgers, The State University of New Jersey, 185 S. Orange Ave., MSB, E-661, Newark, NJ 07103. Tel: +1-973-972-9812; Fax: +1-973-972-1644. yuanxiang.tao@njms.rutgers.edu.

*These authors contributed equally to this study.

AUTHOR CONTRIBUTIONS

Y.X.T. conceived the project and supervised all experiments. L.H., G.H., S.W., S.D. and Y.X.T. assisted with experimental design. L.H., G.H., S.D., S.W., S.D., Y.Z., W.L., B.J., S.X., S.X. and L.Z. carried out animal surgery and molecular, biochemical, morphological, and behavioral experiments. L.H., G.H., S.D., Y.Z., W.L., S.H., Y.X. and Y.X.T. analyzed the data. L.H., Y.X. and Y.X.T. wrote the draft of manuscript. All authors read and discussed the manuscript.

COMPETING FINANCIAL INTERESTS

The authors declare no competing financial interests.

mechanical, thermal and cold stimuli, and induced the spontaneous pain on the ipsilateral side in the absence of SNL. Mechanistically, the increased TLR7 activated the NF-κB signaling pathway through promoting the translocation of p65 into the nucleus and phosphorylation of p65 in the nucleus from the injured DRG neurons. Our findings suggest that DRG TLR7 contributes to neuropathic pain by activating NF-κB in primary sensory neurons. TLR7 may be a potential target for therapeutic treatment of this disorder.

Keywords

Toll like receptor 7; NF-κB pathway; primary sensory neurons; neuropathic pain

Introduction

Neuropathic pain is one of the most serious neurological diseases with an incidence of 3.3–17.9 % in the population (Cohen and Mao, 2014). It is a debilitating neurological condition often caused by injury to the nervous system arising from physical injury, infection, and autoimmune disorders (van et al., 2014). Currently, there are several strategies for neuropathic pain treatment including nonsteroidal anti-inflammatory drugs, opioids, anticonvulsants and antidepressants; however, almost two-thirds of patients do not respond to these treatments, and are considered treatment-resistant (Gaskin and Richard, 2012). Therefore, understanding pathological mechanisms of neuropathic pain is imperative in order to develop novel analgesics for achieving ideal therapeutic efficacy.

Toll-like receptors (TLRs) are a family of transmembrane pattern recognition receptors that mediate innate and adaptive immunity by recognizing exogenous ligands, pathogen-associated molecular patterns and danger-associated molecular patterns (Akira et al., 2006). TLRs are not only expressed in the immune system, but also in neurons and non-neuronal cells (such as astrocytes and microglia) of the nervous system (Barton and Medzhitov, 2003;Ji, 2015). To date, 10 functional TLRs (TLRs 1–10) in humans, and 12 functional TLRs in mice (TLRs1–9; TLRs 11–13) have been identified (Barton and Medzhitov, 2003). Emerging evidence suggests the roles of TLRs in pain and itch. Expression of TLR2, TLR4 and TLR8 in the DRG neurons was upregulated after peripheral nerve injury or diabetic neuropathy (Jurga et al., 2016;Chen et al., 2017;Zhang et al., 2018). Repeated intrathecal administration of LPS-RS (TLR2 and TLR4 antagonist) and LPS-RS Ultrapure (TLR4 antagonist) attenuated the CCI-induced allodynia and hyperalgesia (Jurga et al., 2016). Inhibition of TLR8 in the DRG attenuated SNL-induced pain hypersensitivity (Zhang et al., 2018). TLR3 was also reported in DRG neurons, and involved in itch through activation or transcriptional control of TRPV1 expression (Liu et al., 2012;Min et al., 2014). TLR5 is co-expressed with neurofilament-200 in large-diameter A-fiber neurons of the dorsal root ganglion (DRG) and plays an important role in neuropathic pain induction (Xu et al., 2015). TLR7 was identified in a subset of DRG neurons that are positive for TRPV1, GRP, TRPA1 and MrgprA3 (Liu et al., 2010;Park et al., 2014). Synthetic TLR7 ligands induced rapid inward currents and action potentials in DRG nociceptor neurons (Liu et al., 2010). Upregulation of TLR7 can induce inflammatory and nociceptive response through production of cytokines in mice (Feng et al., 2015;Ichihara et al., 2017;Park et al., 2014),

indicating that TLR7 in nociceptive neurons may serve as a novel pain mediators. However, although mice with TLR7 deficiency showed a reduction in non-histaminergic itch, they displayed intact acute inflammatory pain elicited by intraplantar injection of capsaicin, mustard oil or formalin (5%) in both the first and second phases, as well as carrageenan-induced persistent inflammatory pain and spinal never ligation-induced neuropathic pain (Liu et al., 2010). Interestingly, another study from the same group revealed the inhibition of formalin (0.5%)-induced nociceptive behaviors in the first and second phases in the TLR7 knockout mice (Park et al., 2014). Therefore, the role of TLR7 in persistent pain is still elusive.

In the present study, the role of DRG TLR7 in neuropathic pain was investigated. We first examined whether peripheral nerve injury caused by the fourth lumbar spinal nerve ligation (SNL) increased the expression of TLR7 in the DRG. We then observed whether this increase contributed to the development and maintenance of SNL-induced pain hypersensitivities. We finally explored how this increase participated in SNL-induced neuropathic pain.

Materials and Methods

Animal preparations

CD1 male or female mice (7–8 weeks) were purchased from Charles River Laboratories (Wilmington, MA). Animals were kept in the central housing facility at Rutgers New Jersey Medical School under a standard 12-h light/dark cycle. Water and food pellets were supplied ad libitum. The experimental procedures were approved by the Animal Care and Use Committee at New Jersey Medical School and consistent with the ethical guidelines of the US National Institutes of Health and the International Association for the Study of Pain. To minimize intra- and inter-individual variability of behavioral outcome measures, animals were acclimated for 2–3 days before behavioral testing was carried out. All efforts were made to minimize animal suffering and reduce the number of animals used. The experimenters were blinded to treatment condition during behavioral testing.

Neuropathic pain models

The fourth lumbar (L_4) spinal nerve ligation (SNL) and chronic constriction injury (CCI) models of neuropathic pain in mice were carried out according to previously published methods (Li et al., 2017;Mo et al., 2018;Sun et al., 2019). Briefly, for the SNL model, the fifth lumbar transverse process was identified and then removed. The underlying L_4 spinal nerve was carefully isolated and tightly ligated with a 7–0 silk suture, and transected distal to the ligature. For the CCI model, the exposed sciatic nerve was loosely ligated with 7–0 silk thread at three sites with an interval of about 1 mm proximal to trifurcation of the sciatic nerve. The sham groups underwent identical procedures of the SNL or CCI group, but without the ligature or transection of the respective nerve.

Behavioral tests

Mechanical, cold, and thermal tests, as well as conditional place preference (CPP) test and locomotor performance were carried out as previously described (Zhao et al., 2013;Zhao et

al., 2017;Liang et al., 2016b;Liang et al., 2016a). Each behavioral test for evoked pain was carried out at 30–60 min intervals. Briefly, for mechanical test, the mice were placed individually in a Plexiglas chamber on an elevated mesh screen. The calibrated von Frey filaments (0.07 and 0.4 g, Stoelting Co.) were applied to each hind paw 10 times at intervals of 5 minutes. A quick withdrawal of the paw was regarded as a positive response. Paw withdrawal frequency was calculated by dividing number of paw withdrawal positive responses by 10 trials. For thermal test, the animal was placed in an individual Plexiglas chamber on a glass plate. A beam of light through a hole in the light box of Model 336 Analgesic Meter (IITC Inc. Life Science Instruments. Woodland Hills, CA) through the glass plate was applied into the middle of the plantar surface of each hind paw. The light beam was automatically turned off when the animal withdrew its foot. The paw withdrawal latency was recorded by the length of time between the start of the light beam and the foot withdrawal. Each test was repeated five times at 5-min intervals for the paw on each side. To avoid tissue damage to the hind paw, a cut-off time of 20 s was applied. For cold test, the animal was placed in an individual Plexiglas chamber on the cold aluminum plate (0°C), the temperature of which was monitored continuously by a thermometer. The paw withdrawal latency was recorded as the length of time between the placement of the hind paw on the plate and a flinching of the paw. Each test was repeated three times at 10-min intervals for the paw on the ipsilateral side. To avoid tissue damage, a cut-off time of 20 s was used. For CPP test, mice were first preconditioned with full access to two different Plexiglas chambers connected through an internal door (Med Associates Inc.) for 30 min. At the end of the preconditioning phase, the basal duration time spent in each chamber was recorded within 15 min. The conditioning protocol was performed for the following 3 days with the internal door closed. The mice first received intrathecal injection of saline (5 μl) specifically paired with one conditioning chamber in the morning. Six hours later, lidocaine (0.8 % in 5 μl of saline) was given intrathecally, paired with another conditioning chamber in the afternoon. The injection order of saline and lidocaine was switched each consecutive day. On the test day, the mice were placed in one chamber with free access to both chambers. The duration of time that each mouse spent in each chamber was recorded for 15 min. Difference scores were calculated by subtracting preconditioning time from test time spent in the lidocaine chamber. Finally, locomotor function, including placing, grasping, and righting reflexes, was examined. (1) Placing reflex: the placed positions of the hind limbs were slightly lower than those of the forelimbs, and the dorsal surfaces of the hind paws were brought into contact with the edge of a table. Whether the hind paws were placed on the table surface reflexively was recorded; (2) Grasping reflex: After the animal was placed on a wire grid, whether the hind paws grasped the wire on contact was recorded; (3) Righting reflex: when the animal was placed on its back on a flat surface, whether it immediately assumed the normal upright position was recorded. Each trial was repeated five times with 5-min interval and the scores for each reflex were recorded based on counts of each normal reflex.

Formalin test

The formalin test was carried out as described previously(Cui et al., 2016;Liaw et al., 2008). In brief, the mouse received a 10 μl intraplantar injection of 0.5% formalin on one side. After the injection, the duration of licking and lifting was recorded immediately in 5 min periods for 60 min. The first phase response was defined as the total duration of licking and

lifting during the first 10 minutes and the second phase response as the total number of licking and lifting that occurred 10–60 minutes after the injection.

DRG microinjection

DRG microinjection was carried out as described previously (Wu et al., 2019;Huang et al., 2019). Briefly, a dorsal midline incision was made in the lower lumbar region. The left L4 articular processes were exposed and then removed. After the DRG was exposed, the adeno-associated virus (AAV) viral solution (1 μl, 2×10^{13} copies/mL) was injected into the left L4 DRG with a glass micropipette connected to a Hamilton syringe. The pipette was removed 10 min after injection. The surgical field was irrigated with sterile saline, and the skin incision closed with wound clips.

Cell culture and transfection

DRG neuronal cultures were prepared according to previously described methods (Mao et al., 2019;Lutz et al., 2018). For primary DRG neuronal cultures, after 3-week-old male CD1 mice were euthanized with isoflurane, all DRGs were collected in cold Neurobasal Medium (Gibco/ThermoFisher Scientific) with 10% fetal bovine serum (JR Scientific, Woodland, CA), 100 units/ml Penicillin, and 100 μg/ml Streptomycin (Quality Biological, Gaithersburg, MD). The DRGs were then treated with enzyme solution [5 mg/ml dispase, 1 mg/ml collagenase type I in Hanks' balanced salt solution (HBSS) without Ca^{2+} and Mg^{2+} (Gibco/ ThermoFisher Scientific)]. After trituration and centrifugation, dissociated cells were resuspended in mixed Neurobasal Medium and plated in a six-well plate coated with 50 μg/ml poly-D-lysine (Sigma, St. Louis, MO). The cells were incubated at 95% O_2, 5% CO_2, and 37°C. For viral infection, 10 μl of AAV-shRNA-TLR7 (titer ≥ 1×10^{13}/μl) or 8 μl of AAV-TLR7 (titer ≥ 1×10^{13}/μl) was added to each 2 ml well after 24 hours of incubation. Three days later, the cells were collected.

Western blot analysis

Unilateral L_4 DRGs from four mice were pooled together to achieve enough proteins. The tissues were homogenized and the cultured cells ultrasonicated in chilled lysis buffer (10 mM Tris, 1 mM phenylmethylsulfonyl fluoride, 5 mM $MgCl_2$, 5 mM EGTA, 1 mM EDTA, 1mM DTT, 40 μM leupeptin, 250 mM sucrose). Approximately 10% of the homogenates in volume were used for total proteins. The remaining was centrifuged at 4°C for 15 min at 1,000 g. The supernatant was collected for cytosolic proteins and the pellet for nuclear proteins. After the concentrations of the proteins were measured using the Bio-Rad protein assay (Bio-Rad), equal amount of total proteins were heated at 99°C for 5 min and loaded onto a 4–15% stacking/7.5% separating SDS-polyacrylamide gel (Bio-Rad). The proteins were then electrophoretically transferred onto a polyvinylidene difluoride membrane (Bio-Rad). The membrane was first blocked with 3% nonfat milk in Tris-buffered saline containing 0.1% Tween-20 for 1 h at room temperature, and then incubated at 4°C overnight with the following primary antibodies: rabbit anti-TLR7 (1:500; Abcam), rabbit anti-TLR8 (1:500; CST), mouse anti-NF-κB p65 (1:1,000; CST), mouse anti-phosphorylated (p)-NF-κB p65 (Ser536; 1:1000; CST), rabbit anti-GAPDH (1:2,000; Santa Cruz), rabbit anti-H3 (1:1,000; Santa Cruz), mouse anti-GFAP (1:1,000; Abcam), rabbit anti-phosphorylated ERK (p-ERK; 1:1,000; CST), rabbit anti-total ERK (1:1000; CST) and rabbit anti-TRPA1

(1:2,000; Invitrogen). The proteins were detected by horseradish peroxidase-conjugated anti-mouse or anti-rabbit secondary antibody (1:3,000; Jackson ImmunoResearch), visualized by western peroxide reagent and luminol/enhancer reagent (Clarity Western ECL Substrate, Bio-Rad) and exposed using ChemiDoc XRS System with Image Lab software (Bio-Rad). The intensity of blots was quantified with densitometry using Image Lab software (Bio-Rad). All cytosol protein bands were normalized to GAPDH, whereas all nucleus protein to total histone H3.

Quantitative real-time RT-PCR

Unilateral L_4 DRGs from four mice were collected rapidly and pooled together to achieve enough RNA. Total RNA was extracted by miRNeasy kit (Qiagen, Valencia, CA) according to manufacturer's instructions. The reverse-transcription was achieved using ThermoScript Reverse Transcriptase (Invitrogen/Thermo Fisher Scientific) with oligo (dT) primers (Invitrogen/Thermo Fisher Scientific). Template (1 μl) was amplified in a Bio-Rad CFX96 real-time PCR system using specific primers listed in Table 1. Each sample was run in triplicate in a 20 μl reaction volume containing 250 nM forward and reverse primers, 10 μl of Advanced Universal SYBR Green Supermix (Bio-Rad Laboratories), and 20 ng of cDNA. The PCR amplification consisted of 30 s at 95°C, 30 s at 60°C, 30 s at 72°C, and 5 min at 72°C for 39 cycles. Ratios of ipsilateral-side mRNA levels to contralateral-side mRNA levels were calculated using the ΔCt method ($2^{-\Delta\Delta Ct}$) after normalization to *Tuba-1a*, as it has been demonstrated to be stable even after peripheral nerve injury insult in mice (Liang et al., 2016b;Liang et al., 2016a;Wu et al., 2019;Huang et al., 2019;Mao et al., 2019;Lutz et al., 2018).

Immunohistochemistry

Mice were anesthetized with isoflurane and perfused with 100 ml of 4% paraformaldehyde in 0.1 M phosphate-buffered saline (PBS; pH 7.4). After perfusion, the DRGs were dissected, postfixed at 4°C for 4 hours and cryoprotected in 30% sucrose overnight. The sections were cut on a cryostat at a thickness of 20 μm and collected from each DRG by grouping every third section. After being blocked for 1 hour at room temperature in PBS containing 5% goat serum and 0.3% TritonX-100, the sections from naive mouse DRGs were incubated with rabbit anti-TLR7 (1:250, Abcam), mouse anti-NeuN (1:50, GeneTex, Irvine, CA), mouse anti-NF200 (1:200, Sigma), biotinylated IB4 (1:200, Sigma), and mouse anti-CGRP (1:200, Abcam), mouse anti-glutamine synthetase (1:1000, Sigma), or mouse anti-NF-κB p65 (1:1,000, CST) at 4 overnight. The sections from the ipsilateral L_4 DRGs of SNL or sham mice were incubated only with rabbit anti-°C TLR7 (1:250, Abcam) at 4°C overnight. All sections were incubated with species-appropriate fluro-488- or Cy3-conjucted secondary antibody (1:500, Jackson ImmunoResearch), or with FITC-labeled Avidin D (1:200, Sigma) for 2 hours at room temperature. Control experiments included substitution of mouse serum or rabbit serum for the primary antiserum and omission of the primary antiserum. The sections were finally mounted using VectaMount permanent mounting medium (Vector Laboratories, Burlingame, CA) or Vectashield plus 4', 6-diamidino-2-phenylindole (DAPI) mounting medium (Vector Laboratories). The images were taken with a Leica DMI4000 fluorescence microscope (Leica) with DFC365 FX camera (Leica), and

analyzed using NIH Image J software after the contrast of the image were adjusted in the same way.

Plasmid construction and virus production

A *TLR7* shRNA duplex was designed corresponding to bases 13–36 of the mouse *Tlr7* mRNA (GenBank accession number NM_001139511.1). The oligonucleotides harboring the shRNA sequences were synthesized and annealed. A mismatch shRNA with a scrambled sequence and no homology to a mouse gene (scrambled shRNA) was used as a control. The fragments were ligated into the pro-viral plasmid (pAAV5-U6-shRNA) by BamH1/XbaI restriction sites. To construct the plasmid that expresses TLR7 protein, the full-length sequences of *Tlr7* mRNA from mouse DRG were reverse-transcribed and amplified by PCR and primers (Table 1). The achieved segment was digested by BspEI and NotI, and then inserted into the pro-viral plasmid (pAAV5-MCS). The recombinant clones were verified using DNA sequencing. The AAV-DJ viral particles were prepared using AAV-DJ Helper Free Packaging System (Cell Biolabs, Inc., San Diego, CA). The AAV particles were purified using AAV pro Purification Kit (Takara, Mountain View, CA).

Statistical analysis

Animals were assigned into various treatment groups randomly. All results are expressed as means ± S.E.M. One-way or two-way analysis of variance (ANOVA) with repeated measures followed by *post hoc* Tukey testing and paired or unpaired Student's t-test were applied for normally distributed data. While the Mann-Whitney U-test was used for non-parametric data (SigmaPlot 12.5, San Jose, CA). Significance was set at $P < 0.05$.

Results

TLR7 expression is increased in the injured DRG neurons after nerve injury

To explore the potential role of DRG TLR7 in neuropathic pain, we examined whether TLR7 expression was altered in DRG and spinal cord following unilateral L_4 SNL. SNL, but not sham surgery, led to the time-dependent increases in expression of *Tlr7* mRNA and its protein in the ipsilateral L_4 (injured) DRG on days 3, 7, and 14 post-SNL (Fig. 1a and 1b). The ratios of ipsilateral to contralateral *Tlr7* mRNA were increased by 3.6- to 6.7-fold from day 3 to day 14 after SNL, as compared to those at corresponding time points after sham surgery, respectively (Fig. 1a). Consistently, the levels of TLR7 protein were increased by 2.07-fold on day 3, 3.01-fold on day 7 and 1.89-fold on day 14 after SNL compared to naive mice (Fig. 1b). Neither SNL nor sham surgery altered basal expression of *Tlr*7 mRNA (data not shown) and protein in the contralateral L_4 DRG (data not shown), ipsilateral L3 (intact) DRG (Fig.1c) or ipsilateral L_4 spinal cord (Fig. 1c). Similar results were found after CCI to unilateral sciatic nerve. The amount of TLR7 protein was increased 2.2-fold on day 7 after CCI, as compared to the corresponding sham surgery group (Fig. 1d).

We also analyzed the distribution pattern of TLR7, and the change in number of TLR7-positive cells in the DRG following SNL. The double-labeling immunohistochemistry revealed that TLR7 co-expressed with NeuN (a specific neuronal marker), but not glutamine synthetase (GS, a marker for satellite glial cells), in individual cells of the DRG (Fig. 2a and

2b), indicating that TLR7 was expressed exclusively in DRG neurons. Approximately 33.1% of DRG neurons (98 of 296) were positive for TLR7, of which about 36.8% were positive for calcitonin gene-related peptide (CGRP, a marker for small DRG peptidergic neurons; Fig. 2c), 37.2 % for isolectin B4 (IB4, a marker for small non-peptidergic neurons; Fig. 2d) and 35.9 % for neurofilament-200 (NF200, a marker for medium/large cells and myelinated Aβ-fibers; Fig. 2e). Consistently, the cross-sectional area analysis of neuronal somata showed that about 54.8 % of TLR7-labelled neurons were small (< 300 μm^2 in area), 24.4 % were medium (300–600 μm^2 in area), and 20.8 % were large (> 600 μm^2 in area) (Fig. 2f). As expected, the number of TLR7-positive neurons in the ipsilateral L4 DRG on day 7 after SNL was increased by 1.80-fold when compared to the corresponding sham group (Fig. 2g). These findings suggest that *Tlr7* gene can be activated exclusively in the injured DRG neurons in response to peripheral nerve injury.

Blocking increased TLR7 in the injured DRG attenuated the development of SNL-induced pain hypersensitivities

We next asked whether SNL-induced increase in DRG TLR7 contributed to SNL-induced pain hypersensitivity. To this end, we pre-microinjected AAV5 that expressed TLR7 shRNA (AAV5-TLR7 shRNA) into the ipsilateral L4 DRG to block the SNL-induced increase of TLR7 in the injured DRG. AAV5 that expressed control scrambled shRNA (AAV5-scrambled shRNA) was used as a control. As expected, the level of TLR7 protein was significantly increased in the ipsilateral L4 DRGs on day 14 after SNL in AAV5-scrambled shRNA-treated SNL male mice (Fig. 3a). However, this increase was not seen in the AAV5-TLR7 shRNA-treated SNL male mice (Fig. 3a). Neither virus altered basal expression of TLR8 in the ipsilateral L_4 DRG of SNL or sham male mice (Fig. 3a), or basal expression of TLR7 in the contralateral L_4 DRG (data not shown), ipsilateral L3 DRG and ipsilateral L4 spinal cord (Fig. 3b) of SNL or sham male mice.

We further observed the behavioral responses of these SNL or sham male mice after pre-microinjection of virus. Consistent with previous studies (Liang et al., 2016b;Liang et al., 2016a;Wu et al., 2019;Huang et al., 2019), SNL produced long-term mechanical allodynia, thermal hyperalgesia, and cold allodynia on the ipsilateral side in AAV5-scrambled shRNA-microinjected SNL male mice (Fig. 3c–f). The paw withdrawal frequencies in response to 0.07 g and 0.4g von Frey filament stimuli applied to the ipsilateral hindpaw were significantly increased on days 3, 5, 7, 10 and 14 after SNL as compared to pre-injury baseline values (Fig. 3c–d). The paw withdrawal latencies of the ipsilateral hindpaw in response to heat and cold were markedly reduced on days 3, 5, 7, 10 and 14 after SNL (Fig. 3e–f). DRG pre-microinjection of AAV5-TLR7 shRNA into the ipsilateral L_4 DRG greatly blocked the SNL-induced increases in paw withdrawal frequencies to 0.07 g and 0.4 g von Frey filament stimuli, and the SNL-induced decreases in paw withdrawal latencies to thermal and cold stimuli from days 3 to 14 post-SNL (Fig. 3c–f). DRG pre-microinjection of neither virus affected basal paw responses to mechanical, heat, or cold stimuli on the contralateral side of SNL male mice, and on both ipsilateral and contralateral sides of sham male mice during the observation period (Fig. 3c–i). In addition, these SNL or sham male mice with DRG pre-microinjection of either AAV5-TLR7 shRNA or AAV5-scrambled shRNA displayed normal locomotor activity (Table 2). In addition, formalin-induced

increases in duration of licking and lifting in both first and second phases were significantly decreased in the AAV5-TLR7 shRNA-treated male mice as compared to the AAV5-scrambled shRNA-treated male mice 5 weeks after viral microinjection (Fig. 3j). Similar behavioral responses were observed in the female SNL or sham mice after pre-microinjection of AAV5-TLR7 shRNA or AAV5-scrambled shRNA (Fig. 4a–g; Table 2).

We also examined whether DRG pre-microinjection of AAV5-TLR7 shRNA affected the SNL-induced dorsal horn central sensitization as indicated by increases in the phosphorylation of extracellular signal regulated kinase 1/2 (ERK1/2) and glial fibrillary acidic protein (GFAP) in the dorsal horn of male mice. In line with previous studies (Liang et al., 2016a;Wu et al., 2019;Huang et al., 2019), the levels of the phosphorylation of ERK1/2 (but not total ERK1/2) and GFAP were significantly increased in the ipsilateral L_4 dorsal horn on day 14 after SNL in the AAV5-scambled shRNA-microinjected SNL mice, but not in those that received sham surgery (Fig. 5a–b). These increases were absent in the AAV5-TLR7 shRNA-microinjected SNL mice (Fig. 5a–b). Neither AAV5-TLR7 shRNA nor AAV5-scrambled shRNA altered basal expression of phosphorylation of ERK1/2, total ERK1/2 or GFAP in the dorsal horn of sham mice (Fig. 5a–b). Taken together, our results indicate that the increased TLR7 in the injured DRG may be required for the development of SNL-induced pain hypersensitivity and dorsal horn central sensitization.

Blocking increased TLR7 in the injured DRG attenuated the maintenance of SNL-induced pain hypersensitivities

To examine the role of DRG TLR7 in the maintenance of SNL-induced pain hypersensitivities, we subjected male mice to SNL 2 weeks after DRG microinjection of virus into the ipsilateral L_4 DRG, as AAV5 took at least 3–4 weeks to be expressed. Mechanical, thermal and cold hypersensitivities were completely developed in both the AAV5-TLR7 shRNA-microinjected and AAV5-scrambled shRNA-microinjected mice on days 3–5 after SNL (Fig. 6a–d). However, the mechanical and cold allodynia were significantly alleviated on days 14 and 21 post-SNL, and thermal hyperalgesia was markedly mitigated on days 7 to 21 post-SNL in the AAV5-TLR7 shRNA-microinjected mice, as compared to those in the AAV5-scrambled shRNA-microinjected mice (Fig. 6a–d). As expected, neither virus changed basal responses to mechanical, thermal and cold stimuli on the contralateral side of SNL mice (Fig. 6a–d). SNL increased the expression of TLR7 protein by 1.88-fold of the value from naive mice in the ipsilateral L_4 DRG on day 21 post-SNL in the AAV5-scambled shRNA-microinjected SNL mice (Fig. 6e), but this increase was not seen in the AAV5-TLR7 shRNA-microinjected mice (Fig. 6e). Moreover, SNL-induced increases in the levels of the phosphorylated ERK1/2 (but not total ERK1/2) and GFAP in the ipsilateral dorsal horn on day 21 post-SNL from the AAV5-scambled shRNA-microinjected SNL mice were not observed in the AAV5-TLR7 shRNA-microinjected mice (Fig. 6f–g). The evidence revealed an important role of the increased DRG TLR7 in the maintenance of SNL-induced pain hypersensitivities and dorsal horn central sensitization.

DRG overexpression of TLR7 led to neuropathic pain symptoms

To further determine whether the increased DRG TLR7 was sufficient for neuropathic pain, we microinjected AAV5 that expressed full-length TLR7 protein (AAV5-TLR7) into

unilateral L_3 and L_4 DRGs of naive adult mice. AAV5 expressing green fluorescent protein (AAV5-GFP) was used as a control. In line with our expectation, the dramatic increases in the amounts of TLR7 and TRPA1 (a TLR7-coupled protein(Park et al., 2014)) were detected in the injected DRG 8 weeks after microinjection of AAV5-TLR7 compared with microinjection of AAV5-GFP (Fig. 7a). Mice microinjected with AAV5-TLR7, but not AAV5-GFP, displayed significant increases in paw withdrawal frequencies in response to 0.07 g and 0.4 g von Frey filament stimuli (Fig. 7b–c) and marked decreases in paw withdrawal latencies in response to thermal and cold stimuli (Fig. 7d–e) on the ipsilateral side. These changes occurred 4 weeks post-microinjection and persisted for at least 8 weeks (Fig. 7a–e), consistent with the 3–4 week lag period of AAV5 expression, which lasted for at least 3 months (Mo et al., 2018;Li et al., 2017;Zhao et al., 2013). Neither virus affected locomotor function (Table 2) or basal contralateral paw withdrawal responses (Fig. 7b–e). Additionally, we carried out a conditional place preference (CPP) paradigm, and showed that mice microinjected with AAV5-TLR7 (but not AAV5-GFP) spent more time in the lidocaine-paired chamber (Fig. 7f–g), indicating stimulation-independent spontaneous pain. These findings revealed that increased TLR7 in the DRG produces both spontaneous and evoked pain hypersensitivities, symptoms of neuropathic pain commonly seen in the clinic.

We also examined whether increased TLR7 in the DRG led to dorsal horn central sensitization. The amounts of the phosphorylated ERK1/2 (but not total ERK1/2) and GFAP in the ipsilateral $L_{3/4}$ dorsal horn were significantly increased on 8 weeks after microinjection of AAV5-TLR7 compared to those after microinjection of AAV5-GFP (Fig. 7h). These findings further support our behavioral observations described above.

Increased TLR7 activated NF-κB pathway in the injured DRG following SNL

How did the increased TLR7 in the injured DRG participate in neuropathic pain? Given that TLR7 activated nuclear factor κB (NF-κB), and subsequently induced the release of inflammatory mediators in immune cells (Hemmi et al., 2002), and that nerve injury-induced NF-κB activation played an important role in neuropathic pain (Huang et al., 2019;Zhang and Chi, 2018;Zhou et al., 2018), we predicted that NF-κB signaling pathway might mediate the role of the increased DRG TLR7 in neuropathic pain. The activation of NF-κB signaling pathway was evidenced by the translocation of p65, a key member of NF-κB family, from cellular cytoplasm to nucleus and phosphorylation of p-65 in nucleus (Bao et al., 2018;Zhang et al., 2017;Tomita et al., 2016). The amounts of p65 and phosphorylated p65 (p-p65) were significantly increased in the nuclear fraction from the ipsilateral L_4 DRG on day 14 after SNL in mice pre-microinjected with AAV5-scrambled shRNA (Fig. 8a), although total level of p-65 protein was not changed in the ipsilateral L_4 DRG from the AAV5-scrambled shRNA-treated mice on day 14 after SNL when compared with the AAV5-scrambled shRNA-microinjected sham mice (Fig. 8a). These increases were absent in the AAV5-TLR7 shRNA-microinjected mice (Fig. 8a). DRG microinjection of AAV5-TLR7-shRNA did not significantly alter basal expression of p65 and p-p65 in the nuclear fraction from the ipsilateral L_4 DRG of sham mice or basal expression of total p65 in the ipsilateral L_4 DRG of sham or SNL mice (Fig. 8a). Furthermore, microinjection of AAV5–TLR7 into unilateral L_3 and L_4 DRGs increased the expression of p65 and p-p65 in the nuclear fraction from the ipsilateral L_3 and L_4 DRGs 8 weeks post-microinjection, when compared with the

AAV5-GFP-microinjected group (Fig. 8b). There was not a marked difference in basal expression of total p65 in the ipsilateral L3 and L4 DRGs between AAV5–TLR7-microinjected and AAV5-GFP-microinjected groups (Fig. 5b). In addition, cultured DRG neurons transduced with AAV5-TLR7, but not with AAV5-GFP, showed significant increases in the levels of p65 and p-p65 in nuclear fraction (Fig. 8d). These increases were attenuated in the cultured neurons co-transduced with AAV5-TLR7-shRNA, but not with AAV5-scrambled-shRNA (Fig. 8d), suggesting that the induction of p65 and p-p65 in nucleus was specific in responses to TLR7. Co-transduction of AAV5-TLR7-shRNA and AAV5-GFP reduced basal levels of p65- and p-p65 in the cultured DRG neurons (Fig. 8d). As expected, basal level of total p65 was not altered in any virus-transduced cultured DRG neurons (Fig. 8d). Finally, the double-labeling immunohistochemistry revealed the co-expression of p65 with TLR7 in naive DRG neurons (Fig. 8e). Collectively, our findings indicate that the nerve injury-induced increase in TLR7 expression may contribute to activation of the NF-κB pathway in the injured DRG neurons under neuropathic pain conditions.

Discussion

Peripheral nerve injury-induced persistent pain hypersensitivities, including spontaneous pain, mechanical allodynia, thermal hyperalgesia and cold allodynia in a pre-clinical mouse model mimic trauma/surgery-induced neuropathic pain in the clinic. Investigating how peripheral nerve injury leads to nociceptive hypersensitivity may provide new avenues for prevention and treatment of this disorder. In the present study, we reported that peripheral nerve injury produced an increase in TLR7 expression at both mRNA and protein levels in the ipsilateral DRG, and that this increase participated in neuropathic pain through the activation of the transcription factor NF-κB pathway in the injured DRG. Our results indicate that TLR7 may be a potential target for therapeutic treatment of peripheral neuropathic pain.

Toll-like receptors are typically expressed in immune cells to regulate innate immunity (Cohen and Mao, 2014). Considerable evidence also demonstrated that TLRs play an important role in the pathogenesis of many peripheral and central nervous system disorders, including chronic pain and itch (Ji, 2015). Indeed, TLRs (e.g., TLRs2–4; TLRs7–9) expressed in DRG neurons usually acted as molecular detectors to monitor exogenous and/or endogenous pathogens that cause pain and itch (Chiu et al., 2012;Due et al., 2012;Liu et al., 2010;Liu et al., 2012;Qi et al., 2011). SNL, CCI or streptozotocin (STZ)-induced diabetic neuropathy increased expression of TLR2, TLR4 and TLR8 in the DRG neurons (Jurga et al., 2016;Chen et al., 2017;Zhang et al., 2018). CCI-, SNL- or STZ-induced neuropathic pain could be impaired in *Tlr8* knockout mice or by repeated intrathecal administration of TLR2 and TLR4 antagonist or TLR4 antagonist (Jurga et al., 2016;Chen et al., 2017;Zhang et al., 2018). TLR3 co-expresses TRPV1 in small DRG neurons, and its activation evoked inward currents and action potentials in DRG neurons, as well as elicited scratching behaviors. These responses were decreased in *Tlr3* knockout mice (Liu et al., 2012). TLR7 is also expressed in a small subpopulation of DRG neurons that are positive for TRPV1, GRP, TRPA1 and MrgprA3 (Liu et al., 2010;Park et al., 2014). Similar to TLR3, TLR7 activation also led to inward currents and action potentials in DRG neurons (Liu et al., 2010).

Intradermal injection of TLR7 ligands produced significant scratching (Liu et al., 2010). Systemic TLR7 knockout reduced non-histaminergic itch, but did not affect capsaicin-, mustard oil- and formalin-induced acute inflammatory pain, carrageenan-induced persistent inflammatory pain and SNL-induced neuropathic pain (Liu et al., 2010). Interestingly, another study from the same group reported that TLR7 knockout mice displayed a reduction in formalin-induced inflammatory pain (Park et al., 2014). Further study demonstrated that TLR7 mediated the extracellular miRNAs-induced inward currents and action potentials in DRG neurons and spontaneous pain by its coupling to TRPA1 (Park et al., 2014). However, whether DRG TLR7 participates in neuropathic pain is still elusive.

The present study revealed that TLR7 was expressed in all types of DRG neurons, although other non-neuronal cells such as the immune cells potentially expressing TLR7 cannot be excluded in the DRG. More importantly, peripheral nerve injury produced increases in the levels of TLR7 mRNA and protein in the ipsilateral DRG. This suggests that *Tlr7* gene is transcriptionally activated under neuropathic pain conditions. How peripheral nerve injury triggers *Tlr7* gene activation in the DRG is unclear, but this activation is likely related to the expression of transcription factors and/or caused by epigenetic modifications or increases in RNA stability (Liang et al., 2016b;Liang et al., 2016a;Sun et al., 2019;Zhao et al., 2017;Zhao et al., 2013). These possibilities will be examined in our future study. We further demonstrated that nerve injury-induced increase in DRG TLR7 contributed to neuropathic pain. DRG microinjection of AAV5-TLR7 shRNA, but not control AAV5-scrambled shRNA, blocked the SNL-induced increase of DRG TLR7 expression, dorsal horn central sensitization and pain hypersensitivities during the development and maintenance periods. Consistent with the previous study(Park et al., 2014), formalin-induced duration of licking and lifting was markedly reduced in both first and second phases after DRG TLR7 knockdown through DRG microinjection of AAV5-TLR7 shRNA. Unlike TLR4 and TLR9(Stokes et al., 2013a;Luo et al., 2019), sex dimorphism was not seen in TLR7 signaling as DRG *Tlr7* knockdown in both male and female SNL mice revealed similar impaired behavioral responses. In addition, DRG overexpression of TLR7 led to neuropathic pain-like symptoms in the mice with the absence of nerve injury. However, a previous study showed that *Tlr7* knockout mice exhibited intact SNL-induced neuropathic pain (Liu et al., 2010). This apparent discrepancy might be the result in the differences between *Tlr7* knockout and knockdown strategies. It bears noting that the use of gene knockout mice may have potential confounding and compensatory issues (O'Dell et al., 1994;Tao et al., 2004). Systemically knocking out *Tlr7* gene very likely results in compensatory changes in the expression of other genes, or non-specific changes during the development period that affect the behaviors in adult mice. In contrast, microinjection of AAV5-TLR7 shRNA into the injured DRG of adult mice does not have developmental compensatory issue. This microinjection specifically and selectively knocked down TLR7 only in the injected (ipsilateral) L_4 DRG, given that basal TLR8 expression was unaffected in the injected DRG and that basal level of TLR7 in the ipsilateral L_3 (intact) DRG and ipsilateral L_4 spinal cord was unaltered after DRG viral microinjection. Consistent with our previous reports (Liang et al., 2016b;Liang et al., 2016a;Mao et al., 2019;Sun et al., 2019;Zhao et al., 2013), DRG microinjection did not cause significant cellular damages in the DRG (data shown). Unexpectedly, DRG microinjection of AAV5-TLR7 shRNA did not markedly affect basal

expression of TLR7 protein in the sham group, although this AAV5-TLR7 shRNA was effective in cultured DRG neurons. Why AAV5-TLR7 shRNA had not effect on basal TLR7 expression in vivo is unclear but could be attributed to lower level of DRG TLT7 expression under normal conditions. AAV5-TLR7 shRNA given at current volume and title likely cannot produce more reduction in DRG TLR7 at baseline.

The NF-κB pathway mediates the function of the increased DRG TLR7 in neuropathic pain. NF-κB, a ubiquitous rapid response transcription factor, is involved in the generation of numerous genes encoding inflammatory cytokines, chemokines and nociceptive mediators, and participates in neuropathic pain genesis (Chen et al., 2016;Guo et al., 2018;Huang et al., 2019;Xu et al., 2017). NF-κB is activated in DRG neurons following peripheral nerve injury (Huang et al., 2019;Yu et al., 2017;Zhang et al., 2013). Intrathecal administration of the NF-κB inhibitor, pyrrolidine dithiocarbamate, relieved neuropathic pain and reduced the production of pro-inflammatory cytokines (TNF-α, IL-1β and IL-6), nerve growth factor and brain-derived neurotrophic factor expression in the DRG (Xu et al., 2017;Yu et al., 2017;Zhang et al., 2013). The present study showed that blocking the increase in DRG TLR7 expression reduced the SNL-induced nuclear translocation of NF-κB subunit p65, as well as the SNL-induced increase of nuclear phosphorylated p65 in the injured DRG. Mimicking the SNL-induced increase in DRG TLR7 through DRG microinjection of AAV5-TLR7 activated the NF-κB signaling pathway, increased the level of TLR7-coupled TRPA1 (Park et al., 2014) in the DRG neurons and led to neuropathic pain-like symptoms in the absence of SNL. The double-labeling assay indicated the co-expression of TLR7 and p65 in individual DRG neurons. These findings strongly suggest that TLR7 is required for the activation of the NF-κB signaling pathway and subsequent production of pre-inflammatory cytokines and other pain-associated factors (and/or channels/receptors, e.g., TRPA1) in the DRG after peripheral nerve injury. Because these cytokines/factors triggers hyper-excitability of DRG neurons and produces more sensitive responses to innocuous and noxious stimuli (Xu et al., 2017;Yu et al., 2017;Zhang et al., 2013), TLR7 may participate in the spontaneous activity of the injured DRG neurons and neuropathic pain genesis. This conclusion is further supported by the evidence that the adaptor myeloid differentiation primary response protein 88 (MyD88) recruited by TLR7 led to NF-κB inhibitor (IκB) phosphorylation, resulting in activation and nuclear translocation of the NF-κB (Thakur et al., 2017). Moreover, MyD88 expression in the DRG neurons was upregulated, and neuropathic pain in MyD88 conditional or genetic knockout mice was reduced after CCI or following chemotherapy (Liu et al., 2016;Liu et al., 2014;Woller et al., 2015;Stokes et al., 2013b). Whether the increased DRG TLR7 following peripheral nerve injury triggers other cellular signals is unknown, but DRG TLR7 contributes to neuropathic pain at least in part through the activation of the NF-κB signaling pathway in the DRG neurons.

In conclusion, we demonstrated that blocking the SNL-induced increase in DRG TLR7 expression alleviated the SNL-induced pain hypersensitivity during the development and maintenance periods, without affecting acute or basal nociceptive responses and locomotor functions. These findings suggest that TLR7 may be a potential target for therapeutic treatment of neuropathic pain. However, it brings our attention that TLR7 is expressed in other tissues in addition to DRG and may target other cellular signaling pathways besides NF-κB. Thus, potential side effects caused by TLR7 knockdown/out should be considered.

Supplementary Material

Refer to Web version on PubMed Central for supplementary material.

ACKNOWLEDGMENTS

This work was supported by NIH grants (R01NS094664, R01NS094224, R01NS111553 and RFNS113881) to Y.X.T.

References

Akira S, Uematsu S, Takeuchi O (2006) Pathogen recognition and innate immunity. Cell 124:783–801. [PubMed: 16497588]

Bao Q, Li C, Xu C, Zhang R, Zhao K, Duan Z (2018) Porcine enterocyte protein Btnl5 negatively regulates NF-kappa B pathway by interfering p65 nuclear translocation. Gene 646:47–55. [PubMed: 29197592]

Barton GM, Medzhitov R (2003) Toll-like receptor signaling pathways. Science 300:1524–1525. [PubMed: 12791976]

Chen T, Li H, Yin Y, Zhang Y, Liu Z, Liu H (2017) Interactions of Notch1 and TLR4 signaling pathways in DRG neurons of in vivo and in vitro models of diabetic neuropathy. Sci Rep 7:14923. [PubMed: 29097792]

Chen Y, Chen X, Yu J, Xu X, Wei X, Gu X, Liu C, Zhang D, Xu Z (2016) JAB1 is Involved in Neuropathic Pain by Regulating JNK and NF-kappaB Activation After Chronic Constriction Injury. Neurochem Res 41:1119–1129. [PubMed: 26700435]

Chiu IM, von Hehn CA, Woolf CJ (2012) Neurogenic inflammation and the peripheral nervous system in host defense and immunopathology. Nat Neurosci 15:1063–1067. [PubMed: 22837035]

Cohen SP, Mao J (2014) Neuropathic pain: mechanisms and their clinical implications. BMJ 348:f7656. [PubMed: 24500412]

Cui L, Miao X, Liang L, Abdus-Saboor I, Olson W, Fleming MS, Ma M, Tao YX, Luo W (2016) Identification of Early RET+ Deep Dorsal Spinal Cord Interneurons in Gating Pain. Neuron 91:1137–1153. [PubMed: 27545714]

Due MR, Piekarz AD, Wilson N, Feldman P, Ripsch MS, Chavez S, Yin H, Khanna R, White FA (2012) Neuroexcitatory effects of morphine-3-glucuronide are dependent on Toll-like receptor 4 signaling. J Neuroinflammation 9:200. [PubMed: 22898544]

Feng Y, Chen H, Cai J, Zou L, Yan D, Xu G, Li D, Chao W (2015) Cardiac RNA induces inflammatory responses in cardiomyocytes and immune cells via Toll-like receptor 7 signaling. J Biol Chem 290:26688–26698. [PubMed: 26363072]

Gaskin DJ, Richard P (2012) The economic costs of pain in the United States. J Pain 13:715–724. [PubMed: 22607834]

Guo D, Hu X, Zhang H, Lu C, Cui G, Luo X (2018) Orientin and neuropathic pain in rats with spinal nerve ligation. Int Immunopharmacol 58:72–79. [PubMed: 29558662]

Hemmi H, Kaisho T, Takeuchi O, Sato S, Sanjo H, Hoshino K, Horiuchi T, Tomizawa H, Takeda K, Akira S (2002) Small anti-viral compounds activate immune cells via the TLR7 MyD88-dependent signaling pathway. Nat Immunol 3:196–200. [PubMed: 11812998]

Huang LN, Zou Y, Wu SG, Zhang HH, Mao QX, Li JB, Tao YX (2019) Fn14 Participates in Neuropathic Pain Through NF-kappaB Pathway in Primary Sensory Neurons. Mol Neurobiol 56:7085–7096. [PubMed: 30976982]

Ichihara K, Aizawa N, Akiyama Y, Kamei J, Masumori N, Andersson KE, Homma Y, Igawa Y (2017) Toll-like receptor 7 is overexpressed in the bladder of Hunner-type interstitial cystitis, and its activation in the mouse bladder can induce cystitis and bladder pain. Pain 158:1538–1545. [PubMed: 28595240]

Ji RR (2015) Neuroimmune interactions in itch: Do chronic itch, chronic pain, and chronic cough share similar mechanisms? Pulm Pharmacol Ther 35:81–86. [PubMed: 26351759]

Jurga AM, Rojewska E, Piotrowska A, Makuch W, Pilat D, Przewlocka B, Mika J (2016) Blockade of Toll-Like Receptors (TLR2, TLR4) Attenuates Pain and Potentiates Buprenorphine Analgesia in a Rat Neuropathic Pain Model. Neural Plast 2016:5238730. [PubMed: 26962463]

Li Z, Mao Y, Liang L, Wu S, Yuan J, Mo K, Cai W, Mao Q, Cao J, Bekker A, Zhang W, Tao YX (2017) The transcription factor C/EBPbeta in the dorsal root ganglion contributes to peripheral nerve trauma-induced nociceptive hypersensitivity. Sci Signal 10.

Liang L, Gu X, Zhao JY, Wu S, Miao X, Xiao J, Mo K, Zhang J, Lutz BM, Bekker A, Tao YX (2016a) G9a participates in nerve injury-induced Kcna2 downregulation in primary sensory neurons. Sci Rep 6:37704. [PubMed: 27874088]

Liang L, Zhao JY, Gu X, Wu S, Mo K, Xiong M, Marie LB, Bekker A, Tao YX (2016b) G9a inhibits CREB-triggered expression of mu opioid receptor in primary sensory neurons following peripheral nerve injury. Mol Pain 12.

Liaw WJ, Zhu XG, Yaster M, Johns RA, Gauda EB, Tao YX (2008) Distinct expression of synaptic NR2A and NR2B in the central nervous system and impaired morphine tolerance and physical dependence in mice deficient in postsynaptic density-93 protein. Mol Pain 4:45. [PubMed: 18851757]

Liu T, Berta T, Xu ZZ, Park CK, Zhang L, Lu N, Liu Q, Liu Y, Gao YJ, Liu YC, Ma Q, Dong X, Ji RR (2012) TLR3 deficiency impairs spinal cord synaptic transmission, central sensitization, and pruritus in mice. J Clin Invest 122:2195–2207. [PubMed: 22565312]

Liu T, Xu ZZ, Park CK, Berta T, Ji RR (2010) Toll-like receptor 7 mediates pruritus. Nat Neurosci 13:1460–1462. [PubMed: 21037581]

Liu XJ, Liu T, Chen G, Wang B, Yu XL, Yin C, Ji RR (2016) TLR signaling adaptor protein MyD88 in primary sensory neurons contributes to persistent inflammatory and neuropathic pain and neuroinflammation. Sci Rep 6:28188. [PubMed: 27312666]

Liu XJ, Zhang Y, Liu T, Xu ZZ, Park CK, Berta T, Jiang D, Ji RR (2014) Nociceptive neurons regulate innate and adaptive immunity and neuropathic pain through MyD88 adapter. Cell Res 24:1374–1377. [PubMed: 25112711]

Luo X, Huh Y, Bang S, He Q, Zhang L, Matsuda M, Ji RR (2019) Macrophage Toll-like Receptor 9 Contributes to Chemotherapy-Induced Neuropathic Pain in Male Mice. J Neurosci 39:6848–6864. [PubMed: 31270160]

Lutz BM, Wu S, Gu X, Atianjoh FE, Li Z, Fox BM, Pollock DM, Tao YX (2018) Endothelin type A receptors mediate pain in a mouse model of sickle cell disease. Haematologica 103:1124–1135. [PubMed: 29545351]

Mao Q, Wu S, Gu X, Du S, Mo K, Sun L, Cao J, Bekker A, Chen L, Tao YX (2019) DNMT3a-triggered downregulation of K2p 1.1 gene in primary sensory neurons contributes to paclitaxel-induced neuropathic pain. Int J Cancer 145:2122–2134. [PubMed: 30684388]

Min H, Lee H, Lim H, Jang YH, Chung SJ, Lee CJ, Lee SJ (2014) TLR4 enhances histamine-mediated pruritus by potentiating TRPV1 activity. Mol Brain 7:59. [PubMed: 25139109]

Mo K, Wu S, Gu X, Xiong M, Cai W, Atianjoh FE, Jobe EE, Zhao X, Tu WF, Tao YX (2018) MBD1 Contributes to the Genesis of Acute Pain and Neuropathic Pain by Epigenetic Silencing of Oprm1 and Kcna2 Genes in Primary Sensory Neurons. J Neurosci 38:9883–9899. [PubMed: 30266739]

O'Dell TJ, Huang PL, Dawson TM, Dinerman JL, Snyder SH, Kandel ER, Fishman MC (1994) Endothelial NOS and the blockade of LTP by NOS inhibitors in mice lacking neuronal NOS. Science 265:542–546. [PubMed: 7518615]

Park CK, Xu ZZ, Berta T, Han Q, Chen G, Liu XJ, Ji RR (2014) Extracellular microRNAs activate nociceptor neurons to elicit pain via TLR7 and TRPA1. Neuron 82:47–54. [PubMed: 24698267]

Qi J, Buzas K, Fan H, Cohen JI, Wang K, Mont E, Klinman D, Oppenheim JJ, Howard OM (2011) Painful pathways induced by TLR stimulation of dorsal root ganglion neurons. J Immunol 186:6417–6426. [PubMed: 21515789]

Stokes JA, Cheung J, Eddinger K, Corr M, Yaksh TL (2013a) Toll-like receptor signaling adapter proteins govern spread of neuropathic pain and recovery following nerve injury in male mice. J Neuroinflammation 10:148. [PubMed: 24321498]

Stokes JA, Cheung J, Eddinger K, Corr M, Yaksh TL (2013b) Toll-like receptor signaling adapter proteins govern spread of neuropathic pain and recovery following nerve injury in male mice. J Neuroinflammation 10:148. [PubMed: 24321498]

Sun L, Gu X, Pan Z, Guo X, Liu J, Atianjoh FE, Wu S, Mo K, Xu B, Liang L, Bekker A, Tao YX (2019) Contribution of DNMT1 to Neuropathic Pain Genesis Partially through Epigenetically Repressing Kcna2 in Primary Afferent Neurons. J Neurosci 39:6595–6607. [PubMed: 31182635]

Tao F, Tao YX, Zhao C, Dore S, Liaw WJ, Raja SN, Johns RA (2004) Differential roles of neuronal and endothelial nitric oxide synthases during carrageenan-induced inflammatory hyperalgesia. Neuroscience 128:421–430. [PubMed: 15350652]

Thakur KK, Saini J, Mahajan K, Singh D, Jayswal DP, Mishra S, Bishayee A, Sethi G, Kunnumakkara AB (2017) Therapeutic implications of toll-like receptors in peripheral neuropathic pain. Pharmacol Res 115:224–232. [PubMed: 27894923]

Tomita H, Tabata K, Takahashi M, Nishiyama F, Sugano E (2016) Light induces translocation of NF-kappaB p65 to the mitochondria and suppresses expression of cytochrome c oxidase subunit III (COX III) in the rat retina. Biochem Biophys Res Commun 473:1013–1018. [PubMed: 27055596]

van HO, Austin SK, Khan RA, Smith BH, Torrance N (2014) Neuropathic pain in the general population: a systematic review of epidemiological studies. Pain 155:654–662. [PubMed: 24291734]

Woller SA, Corr M, Yaksh TL (2015) Differences in cisplatin-induced mechanical allodynia in male and female mice. Eur J Pain 19:1476–1485. [PubMed: 25716290]

Wu Q, Wei G, Ji F, Jia S, Wu S, Guo X, He L, Pan Z, Miao X, Mao Q, Yang Y, Cao M, Tao YX (2019) TET1 Overexpression Mitigates Neuropathic Pain Through Rescuing the Expression of mu-Opioid Receptor and Kv1.2 in the Primary Sensory Neurons. Neurotherapeutics 16:491–504. [PubMed: 30515739]

Xu T, Li D, Zhou X, Ouyang HD, Zhou LJ, Zhou H, Zhang HM, Wei XH, Liu G, Liu XG (2017) Oral Application of Magnesium-L-Threonate Attenuates Vincristine-induced Allodynia and Hyperalgesia by Normalization of Tumor Necrosis Factor-alpha/Nuclear Factor-kappaB Signaling. Anesthesiology 126:1151–1168. [PubMed: 28306698]

Xu ZZ, Kim YH, Bang S, Zhang Y, Berta T, Wang F, Oh SB, Ji RR (2015) Inhibition of mechanical allodynia in neuropathic pain by TLR5-mediated A-fiber blockade. Nat Med 21:1326–1331. [PubMed: 26479925]

Yu HM, Wang Q, Sun WB (2017) Silencing of FKBP51 alleviates the mechanical pain threshold, inhibits DRG inflammatory factors and pain mediators through the NF-kappaB signaling pathway. Gene 627:169–175. [PubMed: 28629826]

Zhang HH, Hu J, Zhou YL, Hu S, Wang YM, Chen W, Xiao Y, Huang LY, Jiang X, Xu GY (2013) Promoted interaction of nuclear factor-kappaB with demethylated cystathionine-beta-synthetase gene contributes to gastric hypersensitivity in diabetic rats. J Neurosci 33:9028–9038. [PubMed: 23699514]

Zhang Y, Chi D (2018) Overexpression of SIRT2 Alleviates Neuropathic Pain and Neuroinflammation Through Deacetylation of Transcription Factor Nuclear Factor-Kappa B. Inflammation 41:569–578. [PubMed: 29222643]

Zhang YC, Huo FC, Wei LL, Gong CC, Pan YJ, Mou J, Pei DS (2017) PAK5-mediated phosphorylation and nuclear translocation of NF-kappaB-p65 promotes breast cancer cell proliferation in vitro and in vivo. J Exp Clin Cancer Res 36:146. [PubMed: 29041983]

Zhang ZJ, Guo JS, Li SS, Wu XB, Cao DL, Jiang BC, Jing PB, Bai XQ, Li CH, Wu ZH, Lu Y, Gao YJ (2018) TLR8 and its endogenous ligand miR-21 contribute to neuropathic pain in murine DRG. J Exp Med 215:3019–3037. [PubMed: 30455267]

Zhao JY, Liang L, Gu X, Li Z, Wu S, Sun L, Atianjoh FE, Feng J, Mo K, Jia S, Lutz BM, Bekker A, Nestler EJ, Tao YX (2017) DNA methyltransferase DNMT3a contributes to neuropathic pain by repressing Kcna2 in primary afferent neurons. Nat Commun 8:14712. [PubMed: 28270689]

Zhao X, Tang Z, Zhang H, Atianjoh FE, Zhao JY, Liang L, Wang W, Guan X, Kao SC, Tiwari V, Gao YJ, Hoffman PN, Cui H, Li M, Dong X, Tao YX (2013) A long noncoding RNA contributes to neuropathic pain by silencing Kcna2 in primary afferent neurons. Nat Neurosci 16:1024–1031. [PubMed: 23792947]

Zhou L, Hu Y, Li C, Yan Y, Ao L, Yu B, Fang W, Liu J, Li Y (2018) Levo-corydalmine alleviates vincristine-induced neuropathic pain in mice by inhibiting an NF-kappa B-dependent CXCL1/CXCR2 signaling pathway. Neuropharmacology 135:34–47. [PubMed: 29518397]

Highlights:

1. Peripheral nerve injury led to time-dependently increase in the expression of Toll like receptor 7 (TLR7) at both mRNA and protein levels in mouse injured dorsal root ganglion (DRG).
2. Blocking this increase alleviated the nerve injury-induced mechanical, thermal and cold pain hypersensitivities, and blocked the nerve injury-induced dorsal horn central sensitization during the development and maintenance periods.
3. Mimicking this increase augmented responses to mechanical, thermal and cold stimuli and led to dorsal horn central sensitization in the absence of peripheral nerve injury.
4. The increased TLR7 contributed to neuropathic pain by activating the NF-κB signaling pathway in the DRG neurons.

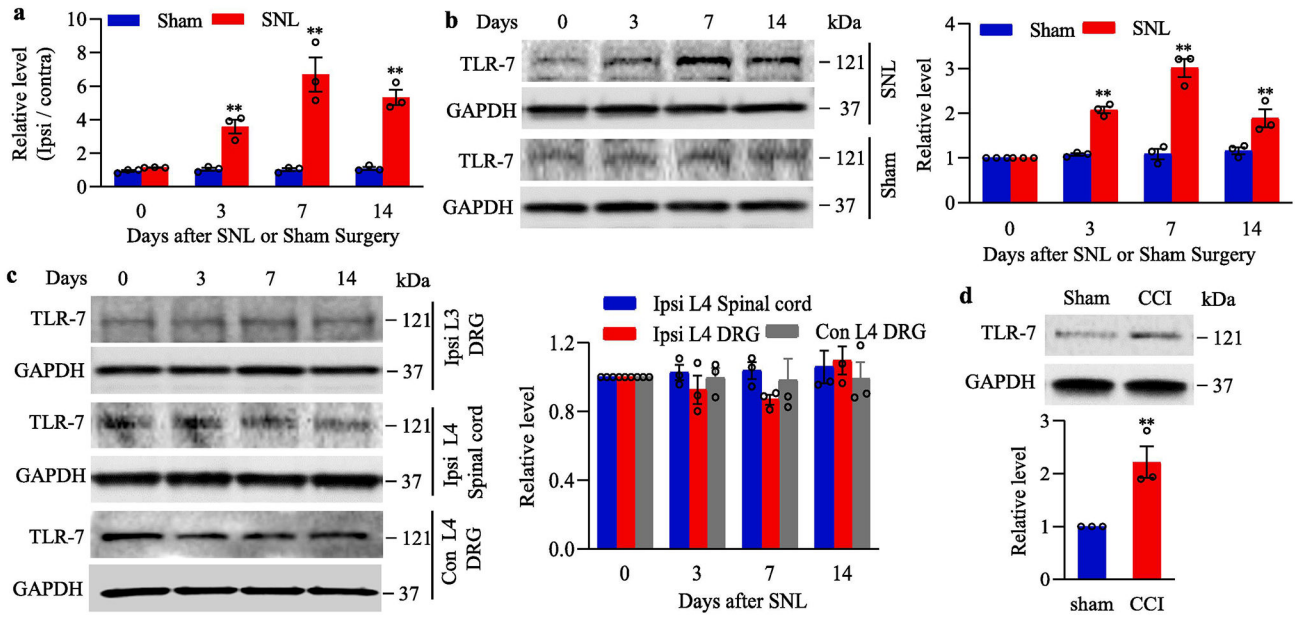

Fig. 1.

Peripheral nerve injury-induced increases in *Tlr7* mRNA and TLR7 protein in the injured dorsal root ganglion (DRG). (a) *Tlr7* mRNA expression in the ipsilateral L_4 DRG of mouse after SNL or sham surgery. n = 3 biological repeats (12 mice)/time point/group. $^{**}P < 0.01$ *vs* the corresponding control group (0 day). Two-way ANOVA with repeated measures followed by post hoc Tukey test. (b) Expression of TLR7 protein in the ipsilateral L_4 DRG of mouse after SNL or sham surgery. Representative Western blots (left panels) and a summary of densitometric analysis (right graphs) are shown. n = 3 biological repeats (12 mice)/time point/group. $^{**}P < 0.01$ *vs* the corresponding control group (0 day). Two-way ANOVA with repeated measures followed by post hoc Tukey test. (c) Expression of TLR7 protein in the ipsilateral L_3 (intact) DRG, contralateral L_4 DRG and ipsilateral L_4 spinal cord of mouse after SNL. Representative Western blots (left panels) and a summary of densitometric analysis (right graphs) are shown. n = 3 biological repeats (12 mice)/time point. (d) Expression of TLR7 protein in the ipsilateral $L_{3/4}$ DRGs on day 7 after CCI or sham surgery. n = 3 biological repeats (6 mice)/group. $^{**}P < 0.01$ *vs* the sham group by two-tailed, independent Student's *t* test. Full-length blots are presented in Supplementary Figure 1.

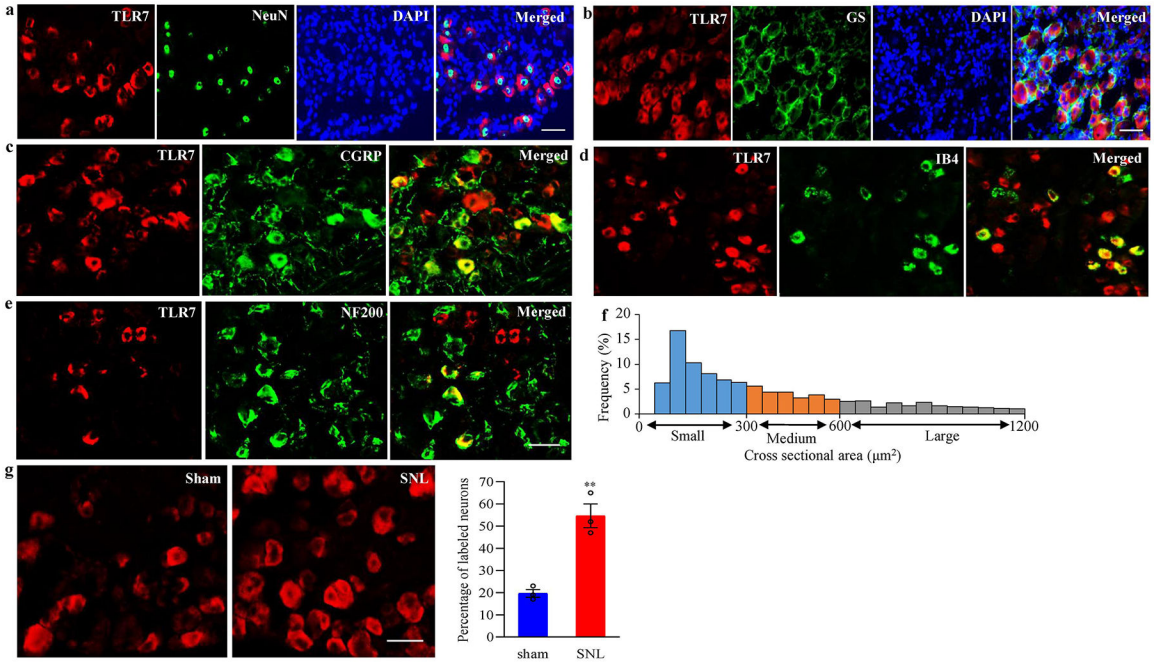

Fig. 2.

Distribution pattern of TLR7 protein in DRG of naive mice and changes in number of TLR7-positive neurons in the injured DRG after SNL. (a, b) Representative examples showing that TLR7 is co-expressed exclusively with NeuN in cellular nuclei (a) and undetected in glutamine synthetase (GS)-labelled cells (b). Cellular nuclei were labeled by 4', 6-diamidino-2-phenylindole (DAPI). n = 3 mice. Scale bars: 50 μm for a and 30 μm for b. (c–e) TLR7-positive neurons were labelled by calcitonin gene-related peptide (CGRP; c), isolectin B4 (IB4; d) or neurofilament-200 (NF200; e) in naive DRG. n = 3 mice. Scale bars: 50 μm. (f) Histogram showing the distribution of TLR7-posirtive neuronal somata in DRG. Small: 55%. Medium: 25%. Large: 20%. (g) Changes in number of TLR7-positive neurons in the ipsilateral L_4 DRG on day 7 after SNL or sham surgery. Representative examples showing the distribution of TLR7-positive neurons (left panels) and a summary of statistical analysis (right graphs). n = 3 mice/group. $^{**}P < 0.01$ *vs* the sham group by two-tailed, independent Student's *t* test. Scale bar: 40 μm.

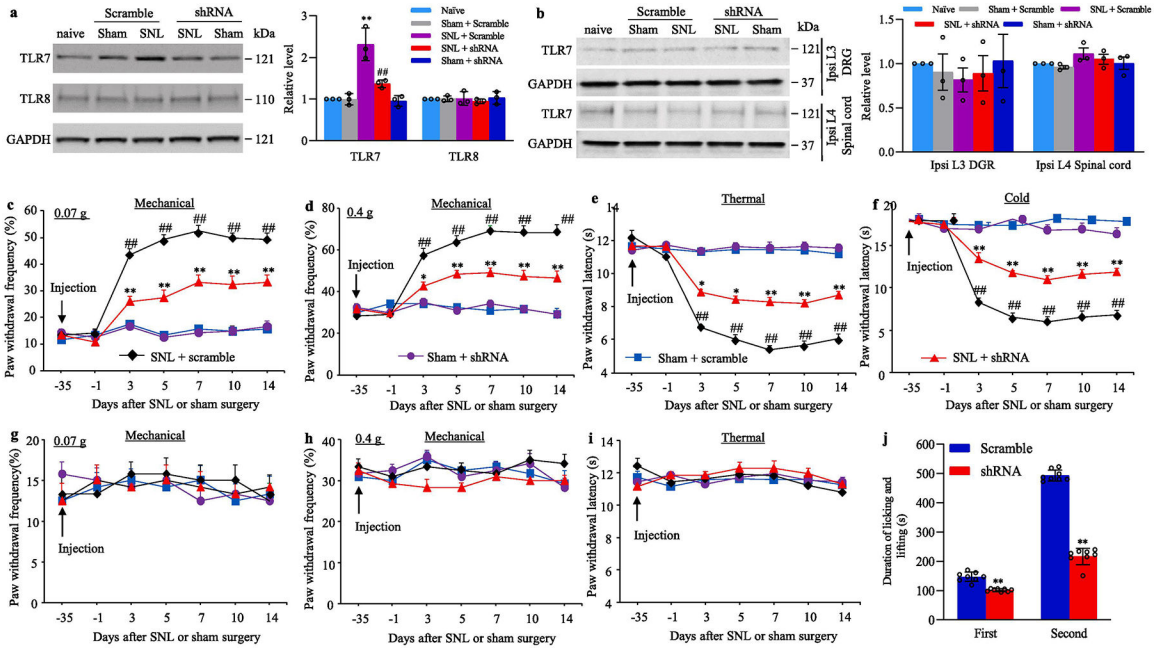

Fig. 3.

Effect of blocking SNL-induced increase in DRG TLR7 protein on SNL-induced development of pain hypersensitivity in male mice. (a, b) The levels of TLR7 and TLR8 proteins in the ipsilateral L_4 DRG (a) and the amount of TLR7 protein in the ipsilateral L_3 DRG and ipsilateral L_4 spinal cord (b) from the AAV5-TLR7 shRNA- or AAV5-scrambled shRNA-microinjected male mice on day 14 post-SNL or sham surgery. n = 3 biological repeats (12 mice)/group. $^{**}P < 0.01$ *vs* the corresponding naive mice. $^{\#\#}P < 0.01$ *vs* the corresponding AAV5-scrambled shRNA-microinjected SNL mice. One-way ANOVA with repeated measures followed by the Tukey post hoc test. (c–i) Paw withdrawal frequency to low (0.07 g; c, g) and median (0.4 g; d, h) force von Frey filament stimuli and paw withdrawal latency to thermal (e, i) and cold (f) stimuli on the ipsilateral side (c–f) and contralateral side (g–i) of male mice with microinjection of AAV5-TLR7 shRNA or AAV5-scrambled shRNA into the ipsilateral L_4 DRG at different days post-SNL or sham surgery. n = 12 mice/group. $^{\#\#}P < 0.01$ *vs* the AAV5-scrambled shRNA-microinjected sham mice at the corresponding time point. $^{*}P < 0.05$ or $^{**}P < 0.01$ *vs* the AAV5-scrambled shRNA-microinjected SNL mice at the corresponding time point. Two-way ANOVA with repeated measures followed by post hoc Tukey test. (j) Duration of licking and lifting in the first and second phases after 0.5% formalin injection into plantar side of the ipsilateral hind paw 5 weeks post-DRG microinjection of AAV5-TLR7 shRNA or AAV5-scrambled shRNA into unilateral $L_{3/4}$ DRGs of male mice. n = 8 mice/group. $^{**}P < 0.01$ *vs* the corresponding AAV5-scrambled shRNA-microinjected group by two-tailed, independent Student's *t* test. Full-length blots are presented in Supplementary Figure 1.

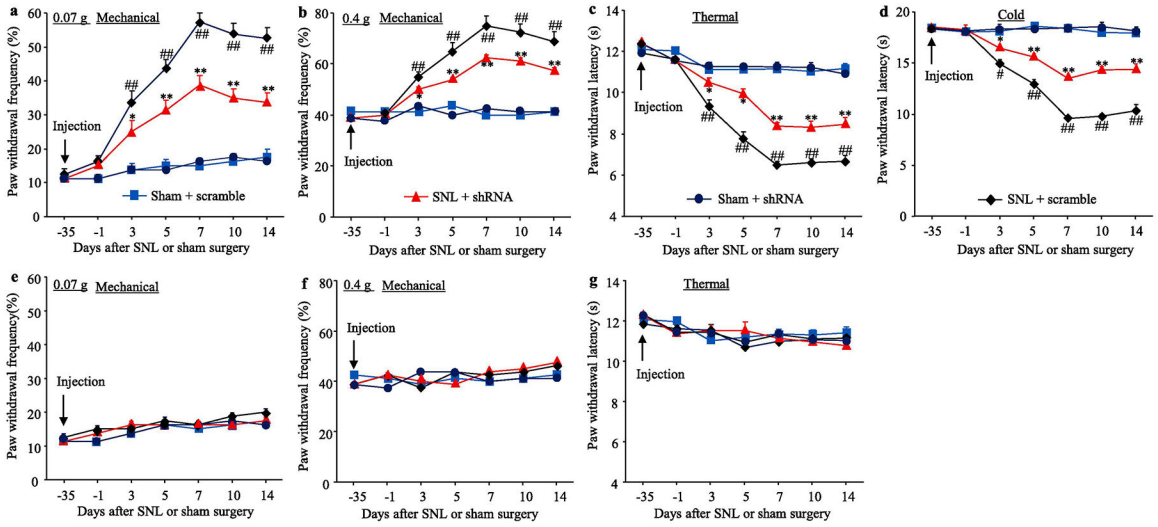

Fig. 4.

Effect of blocking SNL-induced increase in DRG TLR7 protein on SNL-induced development of pain hypersensitivity in female mice. (a–g) Paw withdrawal frequency to low (0.07 g; a, e) and median (0.4 g; b, f) force von Frey filament stimuli and paw withdrawal latency to thermal (c, g) and cold (d) stimuli on the ipsilateral side (a–d) and contralateral side (e–g) of female mice with microinjection of AAV5-TLR7 shRNA or AAV5-scrambled shRNA into the ipsilateral L_4 DRG at different days post-SNL or sham surgery. n = 8 mice/group. $^{\#\#}P < 0.01$ *vs* the AAV5-scrambled shRNA-microinjected sham mice at the corresponding time point. $^{*}P < 0.05$ or $^{**}P < 0.01$ *vs* the AAV5-scrambled shRNA-microinjected SNL mice at the corresponding time point. Two-way ANOVA with repeated measures followed by post hoc Tukey test.

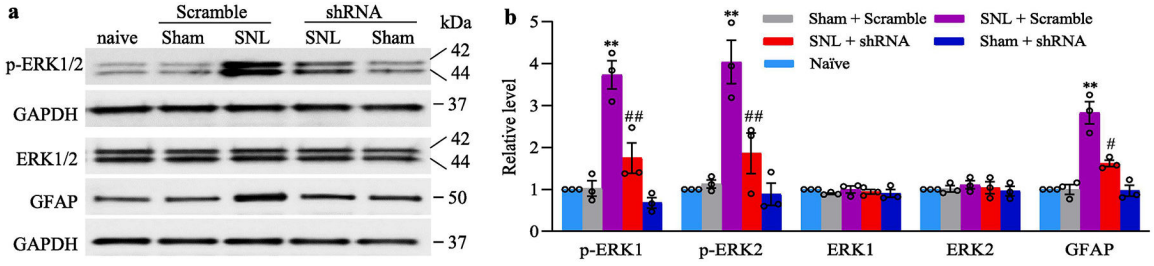

Fig. 5.

Effect of blocking SNL-induced increase in DRG TLR7 protein on the development of dorsal horn central sensitization in male mice, evidenced by the SNL-induced increases in the phosphorylation of ERK1/2 (p-ERK1/2) and abundance of GFAP in the ipsilateral L_4 dorsal horn on day 14 post-SNL or sham surgery. Representative Western blots (a) and a summary of densitometric analysis (b) are shown. n = 3 biological repeats (12 mice)/group. $^{**}P < 0.01$ *vs* the corresponding AAV5-scrambled shRNA-microinjected sham mice. $^{\#}P < 0.05$ or $^{\#\#}P < 0.01$ *vs* the corresponding AAV5-scrambled shRNA-microinjected SNL mice. One-way ANOVA with repeated measures followed by Tukey post hoc test. Full-length blots are presented in Supplementary Figure 1.

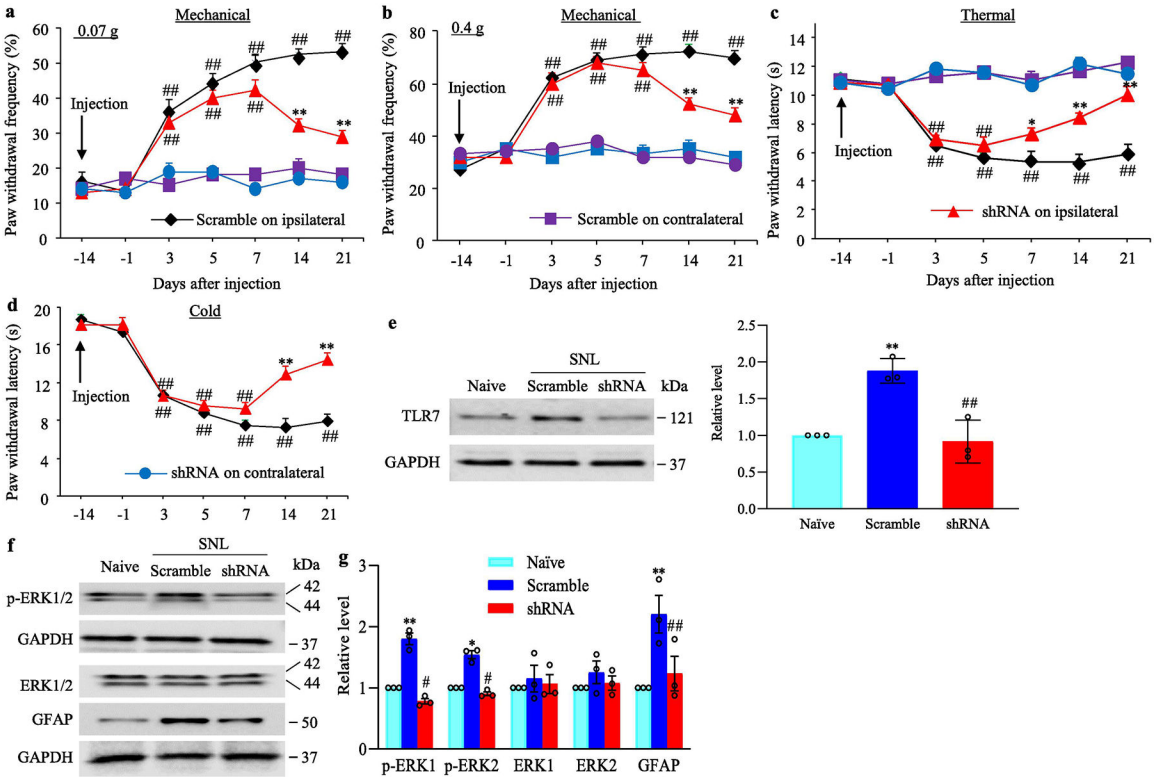

Fig. 6.

Effect of blocking SNL-induced increase in DRG TLR7 on the maintenance of SNL-induced pain hypersensitivity and dorsal horn central sensitization. Male mice were subjected to SNL 14 days after DRG microinjection of AAV5-TLR7 shRNA or AAV5-scrambled shRNA as AAV5 took at least 3–4 weeks to be expressed. (a–d) Paw withdrawal frequency to low (0.07 g; a) and median (0.4 g; b) force von Frey filament stimuli and paw withdrawal latency to thermal (c) and cold (d) stimuli on both ipsilateral and contralateral sides of mice with microinjection of AAV5-TLR7 shRNA or AAV5-scrambled shRNA into the ipsilateral L_4 DRG at different days after SNL. n = 12 mice/group. ## $P < 0.01$ *vs* the corresponding baseline (−14 day). * $P < 0.05$ or ** $P < 0.01$ *vs* the AAV5-scrambled shRNA-microinjected SNL mice at the corresponding time point on the ipsilateral side. Two-way ANOVA with repeated measures followed by post hoc Tukey test. (e) The level of TLR7 protein in the ipsilateral L_4 DRG from the AAV5-TLR7 shRNA- or AAV5-scrambled shRNA-microinjected mice on day 21 post-SNL or sham surgery. n = 3 biological repeats (12 mice)/group. ** $P < 0.01$ *vs* naive mice. ## $P < 0.01$ *vs* the AAV5-scrambled shRNA-microinjected SNL mice. One-way ANOVA with repeated measures followed by Tukey post hoc test. (f.g.) The levels of total ERK1/2, phosphorylation of ERK1/2 (p-ERK1/2) and GFAP in the ipsilateral L_4 dorsal horn on day 21 post-SNL or sham surgery in male mice with pre-DRG microinjection of AAV5-TLR7 shRNA or AAV5-scrambled shRNA. Representative Western blots (a) and a summary of densitometric analysis (b) are shown. n = 3 biological repeats (12 mice)/group. * $P < 0.05$ or ** $P < 0.01$ *vs* the corresponding naive mice. # $P < 0.05$ or ## $P < 0.01$ *vs* the corresponding AAV5-scrambled shRNA-microinjected SNL mice. One-way

ANOVA with repeated measures followed by Tukey post hoc test. Full-length blots are presented in Supplementary Figure 1.

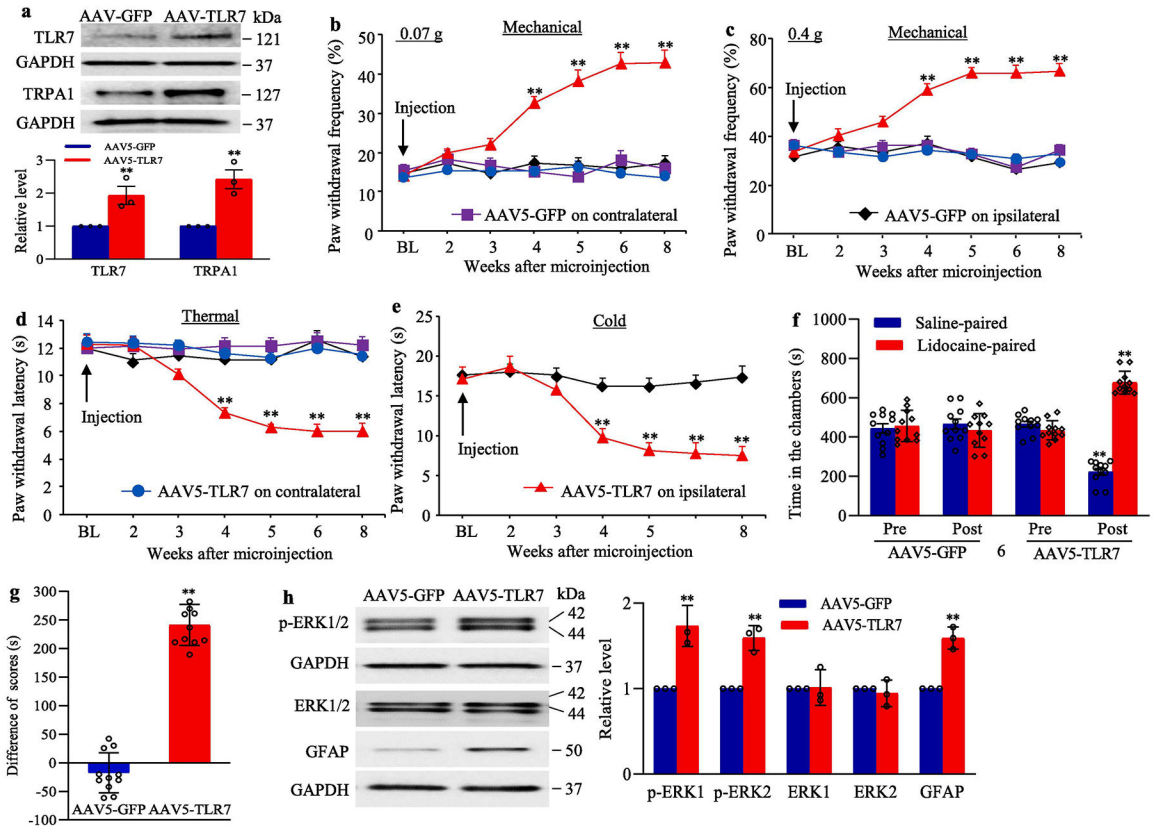

Fig. 7.

Effect of DRG TLR7 overexpression on nociceptive thresholds and dorsal horn central sensitization in naïve mice (a) The levels of TLR7 and TRPA1 proteins in the ipsilateral $L_{3/4}$ DRGs 8 weeks after microinjection of AAV5-TLR7 or control AAV5-GFP. n = 3 biological repeats (6 mice)/group. $^{**}P < 0.01$ *vs* the AAV5-GFP group. Two-tailed, independent Student's *t* test. (b–e) Effect of microinjection of AAV5-TLR7 or AAV5-GFP into the unilateral $L_{3/4}$ DRGs on paw withdrawal frequencies to low (0.07 g; b) and median (0.4 g; c) force von Frey filament stimuli and paw withdrawal latencies to thermal (d) and cold stimuli (e) on both ipsilateral and contralateral sides at the different weeks after AAV5 microinjection. n = 10 mice/group. BL: baseline. $^{**}P < 0.01$ *vs* the control AAV5-GFP group at the corresponding time points on the ipsilateral side. Two-way ANOVA with repeated measures followed by Tukey post hoc test. (f, g) Effect of microinjection of AAV5-TLR7 or AAV5-GFP into the unilateral $L_{3/4}$ DRGs on spontaneous ongoing pain as assessed by the CPP paradigm. n = 10 mice/group. $^{**}P < 0.01$ *vs* the corresponding preconditioning by two-way ANOVA with repeated measures followed by Tukey post hoc test (f) or the AAV5-GFP group by two-tailed, independent Student's *t* test (g). (h) Effect of microinjection of AAV5-TLR7 or AAV5-GFP into the unilateral $L_{3/4}$ DRGs on dorsal horn central sensitization evidenced by the increases in the phosphorylation of ERK1/2 (p-ERK1/2) and abundance of GFAP in the ipsilateral $L_{3/4}$ dorsal horn 8 weeks after viral microinjection. Representative Western blots (left panels) and a summary of densitometric analysis (right graphs) are shown. n = 3 biological repeats (6 mice)/group. $^{**}P < 0.01$ *vs* the

corresponding AAV5-GFP group. Two-tailed, independent Student's *t* test. Full-length blots are presented in Supplementary Figure 1.

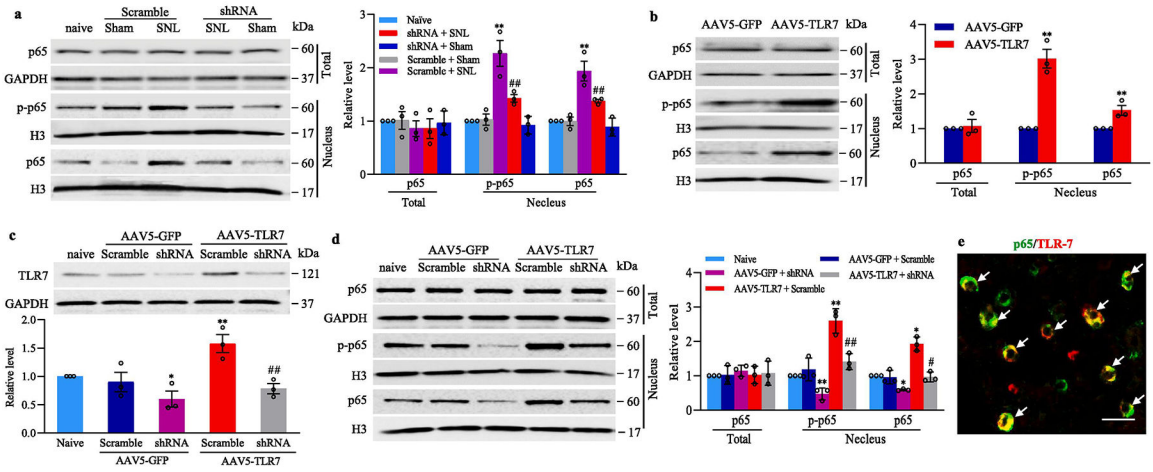

Fig. 8.

TLR7-triggered activation of NF-κB pathway in the injured DRG after SNL. (a) The levels of p-65 in total (cytosolic plus nuclear) fraction and the amounts of p65 and phosphorylated p65 (p-p65) in the nuclear fraction from the ipsilateral L_4 DRG of the mice with microinjection of AAV5-TLR7 shRNA or AAV5-scramble shRNA 14 days after SNL or sham surgery. Representative Western blots (left panels) and a summary of densitometric analysis (right graphs) are shown. n = 3 biological repeats (12 mice)/group. $^{**}P < 0.01$ *vs* the corresponding naive mice. $^{\#\#}P < 0.01$ *vs* the corresponding AAV5-scrambled shRNA-microinjected SNL mice. One-way ANOVA with repeated measures followed by Tukey post hoc test. (b) The amounts of p-65 in total fraction and the levels of p65 and p-p65 in the nuclear fraction in the microinjected $L_{3/4}$ DRGs 8 weeks after microinjection of AAV5-TLR7 or control AAV5-GFP. n = 3 biological repeats (6 mice)/group. Two-tailed, independent Student's *t* test, $^{**}P < 0.01$ *vs* the corresponding AAV5-GFP group. (c, d) The levels of TLR7 (c) and p-65 (d) in total fraction and the amounts of p65 and p-p65 in the nuclear fraction from mouse cultured DRG neurons transduced as indicated. n = 3 biological repeats/treatment. $^{*}P < 0.05$ or $^{**}P < 0.01$ *vs* the corresponding naïve group. $^{\#}P < 0.05$ or $^{\#\#}P < 0.01$ *vs* the corresponding AAV5-TLR7 plus AAV5-scrambled shRNA-treated group. One-way ANOVA with repeated measures followed by Tukey post hoc test. (e) Double labeling staining (arrows) showed co-localization of TLR7 with p65 in mouse L_4 DRG neurons. Scale bar: 40 μm. Full-length blots are presented in Supplementary Figure 1.

Table 1

Primer sequences.

Genes	Sequences (5’ to 3’)
RT qPCR	
Tlr7 F	GGTATGCCGCCAAATCTAAA
Tlr7 R	GCTGAGGTCCAAAATTTCCA
Tubala F	GTGCATCTCCATCCATGTTG
Tubala R	GTGGGTTCCAGGTCTACGAA
Cloning	
Tlr7 RT F	CTCCTCCACCAGACCTCTTG
Tlr7 RT R	TTCCCACCAATCTGAGCCAT
Tlr7 F	TATGGATCCGCCACCATGGTGTTTTCGATGT
Tlr7 R	GCGCTCGAGCTAGACTGTTTCCTTGAACA

RT: Reverse-transcription; F: Forward; R: Reverse.

Table 2:

Locomotor function

Treatment groups	Locomotor function test		
	Placing	Grasping	Righting
AAV5-scramble shRNA + Sham male	5 (0)	5 (0)	5 (0)
AAV5-scramble shRNA + SNL male	5 (0)	5 (0)	5 (0)
AAV5-TLR7 shRNA + Sham male	5 (0)	5 (0)	5 (0)
AAV5-TLR7 shRNA + SNL male	5 (0)	5 (0)	5 (0)
AAV5-GFP in male	5 (0)	5 (0)	5 (0)
AAV5-TLR7 in male	5 (0)	5 (0)	5 (0)
AAV5-scramble shRNA + Sham female	5(0)	5 (0)	5 (0)
AAV5-scramble shRNA + SNL female	5 (0)	5 (0)	5 (0)
AAV5-TLR7 shRNA + Sham female	5 (0)	5 (0)	5 (0)
AAV5-TLR7 shRNA + SNL female	5 (0)	5 (0)	5 (0)

n = 8–12 mice per group; five trials; Mean (SEM)